

Measurement of Branching Fractions for $B \rightarrow \eta_c K^{(*)}$ Decays

F. Fang⁷, T. Hojo³⁰, K. Abe⁸, K. Abe⁴⁰, T. Abe⁴¹, I. Adachi⁸, H. Aihara⁴², M. Akatsu²², Y. Asano⁴⁷, T. Aso⁴⁶, V. Aulchenko¹, A. M. Bakich³⁸, E. Banas²⁶, A. Bay¹⁸, P. K. Behera⁴⁸, I. Bizjak¹³, A. Bondar¹, A. Bozek²⁶, M. Bračko^{20,13}, J. Brodzicka²⁶, T. E. Browder⁷, B. C. K. Casey⁷, P. Chang²⁵, Y. Chao²⁵, K.-F. Chen²⁵, B. G. Cheon³⁷, R. Chistov¹², S.-K. Choi⁶, Y. Choi³⁷, Y. K. Choi³⁷, M. Danilov¹², A. Drutskoy¹², S. Eidelman¹, V. Eiges¹², Y. Enari²², C. Fukunaga⁴⁴, N. Gabyshev⁸, A. Garmash^{1,8}, T. Gershon⁸, B. Golob^{19,13}, T. Hara³⁰, N. C. Hastings²¹, H. Hayashii²³, M. Hazumi⁸, E. M. Heenan²¹, T. Higuchi⁴², L. Hinz¹⁸, T. Hokuue²², Y. Hoshi⁴⁰, W.-S. Hou²⁵, H.-C. Huang²⁵, T. Igaki²², Y. Igarashi⁸, T. Iijima²², K. Inami²², A. Ishikawa²², R. Itoh⁸, H. Iwasaki⁸, Y. Iwasaki⁸, H. K. Jang³⁶, J. H. Kang⁵¹, J. S. Kang¹⁵, P. Kapusta²⁶, N. Katayama⁸, H. Kawai², Y. Kawakami²², T. Kawasaki²⁸, H. Kichimi⁸, D. W. Kim³⁷, Heejong Kim⁵¹, H. J. Kim⁵¹, H. O. Kim³⁷, Hyunwoo Kim¹⁵, S. K. Kim³⁶, K. Kinoshita⁴, S. Kobayashi³⁴, S. Korpar^{20,13}, P. Križan^{19,13}, P. Krokovny¹, R. Kulásíř⁴, Y.-J. Kwon⁵¹, J. S. Lange^{5,33}, G. Leder¹¹, S. H. Lee³⁶, J. Li³⁵, D. Liventsev¹², R.-S. Lu²⁵, J. MacNaughton¹¹, F. Mandl¹¹, S. Matsumoto³, T. Matsumoto⁴⁴, W. Mitaroff¹¹, K. Miyabayashi²³, H. Miyake³⁰, H. Miyata²⁸, G. R. Moloney²¹, T. Mori³, T. Nagamine⁴¹, Y. Nagasaka⁹, T. Nakadaira⁴², E. Nakano²⁹, M. Nakao⁸, H. Nakazawa³, J. W. Nam³⁷, Z. Natkaniec²⁶, S. Nishida¹⁶, O. Nitoh⁴⁵, S. Noguchi²³, T. Nozaki⁸, S. Ogawa³⁹, T. Ohshima²², T. Okabe²², S. Okuno¹⁴, S. L. Olsen⁷, Y. Onuki²⁸, H. Ozaki⁸, P. Pakhlov¹², C. W. Park¹⁵, H. Park¹⁷, K. S. Park³⁷, J.-P. Perroud¹⁸, M. Peters⁷, L. E. Piilonen⁴⁹, F. J. Ronga¹⁸, N. Root¹, M. Rozanska²⁶, K. Rybicki²⁶, H. Sagawa⁸, S. Saitoh⁸, Y. Sakai⁸, H. Sakamoto¹⁶, M. Satapathy⁴⁸, O. Schneider¹⁸, S. Schrenk⁴, C. Schwanda^{8,11}, S. Semenov¹², K. Senyo²², R. Seuster⁷, M. E. Sevior²¹, H. Shibuya³⁹, B. Shwartz¹, V. Sidorov¹, N. Soni³¹, S. Stanič^{47,*}, M. Starič¹³, A. Sugi²², A. Sugiyama²², K. Sumisawa⁸, T. Sumiyoshi⁴⁴, K. Suzuki⁸, S. Suzuki⁵⁰, T. Takahashi²⁹, F. Takasaki⁸, N. Tamura²⁸, J. Tanaka⁴², M. Tanaka⁸, G. N. Taylor²¹, Y. Teramoto²⁹, S. Tokuda²², T. Tomura⁴², K. Trabelsi⁷, T. Tsuboyama⁸, T. Tsukamoto⁸, S. Uehara⁸, K. Ueno²⁵, S. Uno⁸, Y. Ushiroda⁸, S. E. Vahsen³², G. Varner⁷, K. E. Varvell³⁸, C. C. Wang²⁵, C. H. Wang²⁴, J. G. Wang⁴⁹, M.-Z. Wang²⁵, Y. Watanabe⁴³, E. Won¹⁵, B. D. Yabsley⁴⁹, Y. Yamada⁸, A. Yamaguchi⁴¹, Y. Yamashita²⁷, M. Yamauchi⁸, H. Yanai²⁸, J. Yashima⁸, M. Yokoyama⁴², Y. Yuan¹⁰, Y. Yusa⁴¹, C. C. Zhang¹⁰, J. Zhang⁴⁷, Z. P. Zhang³⁵, V. Zhilich¹, and D. Žontar⁴⁷

¹Budker Institute of Nuclear Physics, Novosibirsk²Chiba University, Chiba³Chuo University, Tokyo⁴University of Cincinnati, Cincinnati OH⁵University of Frankfurt, Frankfurt⁶Gyeongsang National University, Chinju⁷University of Hawaii, Honolulu HI⁸High Energy Accelerator Research Organization (KEK), Tsukuba⁹Hiroshima Institute of Technology, Hiroshima¹⁰Institute of High Energy Physics, Chinese Academy of Sciences, Beijing¹¹Institute of High Energy Physics, Vienna¹²Institute for Theoretical and Experimental Physics, Moscow¹³J. Stefan Institute, Ljubljana¹⁴Kanagawa University, Yokohama¹⁵Korea University, Seoul¹⁶Kyoto University, Kyoto¹⁷Kyungpook National University, Taegu¹⁸Institut de Physique des Hautes Énergies, Université de Lausanne, Lausanne¹⁹University of Ljubljana, Ljubljana²⁰University of Maribor, Maribor²¹University of Melbourne, Victoria²²Nagoya University, Nagoya²³Nara Women's University, Nara²⁴National Lien-Ho Institute of Technology, Miao Li²⁵National Taiwan University, Taipei²⁶H. Niewodniczanski Institute of Nuclear Physics, Krakow²⁷Nihon Dental College, Niigata²⁸Niigata University, Niigata²⁹Osaka City University, Osaka³⁰Osaka University, Osaka³¹Panjab University, Chandigarh³²Princeton University, Princeton NJ

³³RIKEN BNL Research Center, Brookhaven NY
³⁴Saga University, Saga
³⁵University of Science and Technology of China, Hefei
³⁶Seoul National University, Seoul
³⁷Sungkyunkwan University, Suwon
³⁸University of Sydney, Sydney NSW
³⁹Toho University, Funabashi
⁴⁰Tohoku Gakuin University, Tagajo
⁴¹Tohoku University, Sendai
⁴²University of Tokyo, Tokyo
⁴³Tokyo Institute of Technology, Tokyo
⁴⁴Tokyo Metropolitan University, Tokyo
⁴⁵Tokyo University of Agriculture and Technology, Tokyo
⁴⁶Toyama National College of Maritime Technology, Toyama
⁴⁷University of Tsukuba, Tsukuba
⁴⁸Utkal University, Bhubaneswar
⁴⁹Virginia Polytechnic Institute and State University, Blacksburg VA
⁵⁰Yokkaichi University, Yokkaichi
⁵¹Yonsei University, Seoul

* on leave from Nova Gorica Polytechnic, Slovenia

We report measurements of branching fractions for charged and neutral $B \rightarrow \eta_c K$ decays where the η_c meson is reconstructed in the $K_S^0 K^\pm \pi^\mp$, $K^+ K^- \pi^0$, $K^{*0} K^- \pi^+$ and $p\bar{p}$ decay channels. The neutral B^0 channel is a CP eigenstate and can be used to measure the CP violation parameter $\sin 2\phi_1$. We also report the first observation of the $B^0 \rightarrow \eta_c K^{*0}$ mode. The results are based on an analysis of 29.1 fb^{-1} of data collected by the Belle detector at KEKB.

PACS numbers: 13.20.He, 13.25.Hw, 13.60.Rj

The decay mode $B \rightarrow \eta_c K$ proceeds by a spectator $b \rightarrow c\bar{c}s$ transition with internal W-emission as in the CP eigenstate $B^0 \rightarrow J/\psi K_S^0$. The neutral decay mode $B^0 \rightarrow \eta_c K_S^0$ has therefore been used to measure the CP violation parameter $\sin 2\phi_1$ [1] [2]. Measurements of branching fractions for $B \rightarrow \eta_c K^{(*)}$ decay modes are also useful in the study of the dynamics of hadronic B decay [3]. However, in contrast to $B^0 \rightarrow J/\psi K_S^0$, the η_c meson must be reconstructed from hadronic decays rather than from a leptonic final state. In this paper, we report new measurements of $B \rightarrow \eta_c K$ branching fractions with the η_c meson reconstructed in the $K_S^0 K^+ \pi^-$, $K^- K^+ \pi^0$, $K^{*0} K^- \pi^+$ and $p\bar{p}$ channels [4]. We also report the first observation of the related decay mode $B^0 \rightarrow \eta_c K^{*0}$. When $K^{*0} \rightarrow K_S^0 \pi^0$, this decay mode is also a CP eigenstate.

We use a 29.1 fb^{-1} data sample, which contains 31.3 million produced $B\bar{B}$ pairs, collected with the Belle detector at the KEKB asymmetric-energy e^+e^- (3.5 on 8 GeV) collider [5]. KEKB operates at the $\Upsilon(4S)$ resonance ($\sqrt{s} = 10.58 \text{ GeV}$) with a peak luminosity that now exceeds $7 \times 10^{33} \text{ cm}^{-2}\text{s}^{-1}$. The Belle detector is a large-solid-angle magnetic spectrometer that consists of a three-layer silicon vertex detector (SVD), a 50-layer central drift chamber (CDC), a mosaic of aerogel threshold Čerenkov counters (ACC), time-of-flight scintillation counters (TOF), and an array of CsI(Tl) crystals (ECL) located inside a superconducting solenoid coil that provides a 1.5 T magnetic field. An iron flux-return located outside of the coil is instrumented to identify K_L and muons (KLM). The detector is described in detail elsewhere [6].

We select well measured charged tracks with impact parameters with respect to the interaction point of less than 0.5 cm in the radial direction and less than 3 cm in the beam direction (z). These tracks are required to have $p_T > 50 \text{ MeV}/c$.

Particle identification likelihoods for the pion and kaon particle hypotheses are calculated by combining information from the TOF and ACC systems with dE/dx measurements in the CDC. To identify kaons (pions), we apply a mode-dependent requirement on the kaon (pion) likelihood ratio, $L_K/(L_\pi + L_K)$ ($L_\pi/(L_\pi + L_K)$). The requirement $L_K/(L_\pi + L_K) > 0.5$ is used for the $\eta_c \rightarrow K_S^0 K^- \pi^+$ mode. For other modes, we require $L_K/(L_\pi + L_K) > 0.6$. This requirement is 88% efficient for kaons with a 8.5% misidentification rate for pions. For the $\eta_c \rightarrow K^+ K^- \pi^0$ mode, the kaon likelihood ratio is required to be greater than 0.8 for those charged kaons that come directly from the B rather than from the η_c candidate. In addition, we remove all kaon candidates that are consistent with being either protons or electrons.

Protons and antiprotons are identified using all particle

ID systems and are required to have proton likelihood ratios ($L_p/(L_p + L_K)$ and $L_p/(L_p + L_\pi)$) greater than 0.4. Proton candidates that are electron-like according to the information recorded by the CsI(Tl) calorimeter are vetoed. This selection is 95% efficient for protons with a 12% kaon misidentification rate.

We select K_S candidates from $\pi^+ \pi^-$ candidates that lie within the mass window $0.482 \text{ GeV}/c^2 < M(\pi^+ \pi^-) < 0.514 \text{ GeV}/c^2$ ($\pm 4\sigma$). The flight length of the K_S is required to be greater than 0.2 cm. The difference in the angle between the vertex direction and the K_S flight direction in the $x - y$ plane is required to satisfy $\Delta\phi < 0.1 \text{ rad}$.

K^{*0} candidates are reconstructed in the $K^+ \pi^-$ mode. For $\eta_c \rightarrow K^{*0} K^- \pi^+$, we require the $K^+ \pi^-$ invariant mass to be between 0.817 and $0.967 \text{ GeV}/c^2$. For the $B^0 \rightarrow \eta_c K^{*0}$ mode, the K^{*0} mass must lie in the range between 0.801 and $0.991 \text{ GeV}/c^2$.

Neutral pion candidates are selected from pairs of ECL clusters with invariant mass within $\pm 16 \text{ MeV}$ of the nominal π^0 mass and momenta above $350 \text{ MeV}/c$. The photons must have energy above 50 MeV if they lie in the barrel region of the calorimeter and above 200 MeV if they are detected in the endcap.

To reconstruct signal candidates in the $B^+ \rightarrow \eta_c K^+$ and $B^0 \rightarrow \eta_c K^0$ modes, we form combinations of charged or neutral kaons and η_c candidates. The η_c is reconstructed in the $K_S^0 K^+ \pi^-$, $K^- K^+ \pi^0$, $K^{*0} K^- \pi^+$ and $p\bar{p}$ decay modes. The η_c candidate is required to have invariant mass in the range $2.920 < M_{\eta_c} < 3.035 \text{ GeV}/c^2$ for the $K^- K^+ \pi^0$ mode and $2.935 < M_{\eta_c} < 3.035 \text{ GeV}/c^2$ for all other modes. The charged daughters of the η_c are required to satisfy a vertex constrained fit with a mode-dependent χ^2 requirement [7].

To isolate the signal, we form the beam-energy constrained mass, $M_{\text{bc}} = \sqrt{E_{\text{beam}}^2 - \vec{P}_{\text{recon}}^2}$, and energy difference $\Delta E = E_{\text{recon}} - E_{\text{beam}}$ in the $\Upsilon(4S)$ center of mass frame. Here E_{beam} , E_{recon} and \vec{P}_{recon} are the beam energy, the reconstructed energy and the reconstructed momentum of the signal candidate, respectively. The signal region for ΔE in all modes except for $\eta_c \rightarrow K_S^0 K^- \pi^+$ is $\pm 2.5\sigma$, where σ is the mode-dependent resolution and ranges from $\pm 25 \text{ MeV}$ for $\eta_c \rightarrow p\bar{p}$ to the range $-55, +45 \text{ MeV}$ for $\eta_c \rightarrow K^- K^+ \pi^0$. In the low background $\eta_c \rightarrow K_S^0 K^- \pi^+$ mode, the region is extended to $\pm 35 \text{ MeV}$, ($\pm 3.5\sigma$). The signal region for M_{bc} is $5.270 \text{ GeV}/c^2 < M_{\text{bc}} < 5.290 \text{ GeV}/c^2$. The resolution in beam-energy constrained mass is $2.8 \text{ MeV}/c^2$ and is dominated by the beam energy spread of KEKB.

Several event topology variables provide discrimination between the large continuum ($e^+e^- \rightarrow q\bar{q}$, where $q = u, d, s, c$) background, which tends to be collimated along the original quark direction, and more spherical

$B\bar{B}$ events. We first remove events with $R_2 > 0.5$, where R_2 is the normalized second Fox-Wolfram moment. We form a likelihood ratio using two variables. Six modified Fox-Wolfram moments and the cosine of the thrust angle are combined into a Fisher discriminant [8]. For signal MC and continuum data, we then form probability density functions for this Fisher discriminant, and the cosine of the B decay angle with respect to the z axis ($\cos\theta_B$). The signal (background) probability density functions are multiplied together to form a signal (background) likelihood \mathcal{L}_S (\mathcal{L}_{BG}). A mode-dependent likelihood ratio requirement $\mathcal{L}_S/(\mathcal{L}_S + \mathcal{L}_{BG})$ is then imposed.

Using a sample of 57 million $B\bar{B}$ Monte Carlo events with a model of all hadronic $b \rightarrow c$ decays, we investigate backgrounds from other B decay modes. In the $\eta_c \rightarrow p\bar{p}$ mode, no such backgrounds are found. In other modes, some background is observed but it can be removed by application of mode-dependent vetos on invariant mass combinations that are consistent with the D , D_s , χ_{c1} , J/ψ , $\psi(2S)$ or $\eta_c(2S)$ masses. For example, in the $B^+ \rightarrow \eta_c K^+$, $\eta_c \rightarrow K^+ K^- \pi^0$ mode, we find there is background from the decay chain $B^+ \rightarrow \bar{D}^0 \rho^+$, $\bar{D}^0 \rightarrow K^- K^+$, $\rho^+ \rightarrow \pi^+ \pi^0$. This background is removed by requiring that the $K^- K^+$ invariant mass be inconsistent with the D^0 mass.

We fit the M_{bc} distribution to the sum of a signal Gaussian and a background function that behaves like phase space near the kinematic boundary [9]. The width of the Gaussian is fixed from MC simulation while the mean is determined from $B^+ \rightarrow \bar{D}^0 \pi^+$ data. The shape parameter of the background function is determined from ΔE sideband data. The signal yield in each mode was determined by fits to M_{bc} . The yields and significances [10] for these fits are given in Table I. Significant signals are observed in all decay modes except for $B^0 \rightarrow \eta_c K^0$, $\eta_c \rightarrow K^{*0} K^- \pi^+$. For this mode, we calculate an upper limit based on the number of events observed in the M_{bc} signal region (4) and the expected number of background events (2) based on the fit. We use the Feldman-Cousins procedure [11], and reduce the efficiency by one sigma of the systematic error in the calculation. The detection efficiencies for all modes were determined from a GEANT based Monte Carlo simulation.

For illustration, in Fig. 1, we show the beam-energy constrained mass and ΔE distributions for the signal candidates in all the decay modes except for $B^0 \rightarrow \eta_c K^0$, $\eta_c \rightarrow K^{*0} K^- \pi^+$. In the M_{bc} distribution, we observe a signal of 195 ± 17 events.

As a consistency check, we also determine the yield from a fit to the ΔE distribution with a double Gaussian for signal and a linear background function with slope determined from the M_{bc} sideband. The results of these fits are also given in Table I. The fit to the ΔE distribution for all modes combined gives a integrated yield of 188 ± 17 events in the signal region. In the fits to the ΔE distribution, the region with $\Delta E < -120$ MeV is ex-

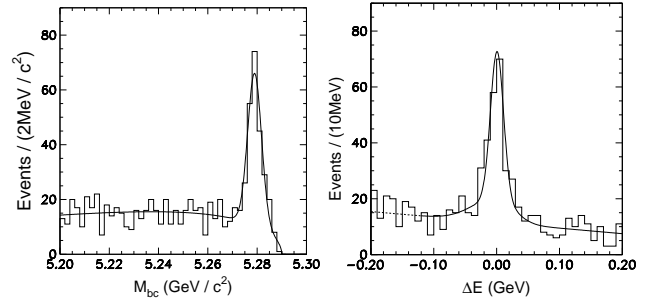


FIG. 1. (a) M_{bc} and (b) ΔE distributions for $B \rightarrow \eta_c K$ candidates in all the decay modes.

cluded to avoid contributions from modes with additional particles such as $B \rightarrow \eta_c K^*$.

After removing the requirements on η_c invariant mass, we also verify that the signal yield for η_c candidates in the M_{bc} , ΔE signal region is consistent with the result used for the branching fraction determination. The η_c invariant mass distribution for signal candidates is shown in Fig. 2. Fitting to a Breit-Wigner convolved with the resolution determined from MC, we find an intrinsic width $\Gamma(\eta_c) = 29 \pm 8 \pm 6$ MeV and a mass $M(\eta_c) = 2979.6 \pm 2.3 \pm 1.6$ MeV. The systematic errors in the width and mass measurements include the effects of varying the background shape, the small difference between data and MC detector resolutions, and possible binning effects. The results are consistent with world averages [12]. The yield is 182 ± 25 events. We also observe a clear signal of 66 ± 18 events from $B \rightarrow J/\psi K$, where the J/ψ is reconstructed in hadronic decay modes, that has a J/ψ mass and yield that are consistent with values obtained for the $J/\psi \rightarrow \ell^+ \ell^-$ decay mode.

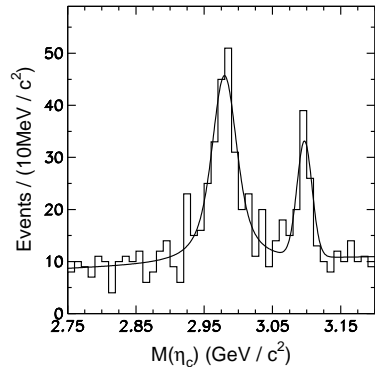


FIG. 2. Candidate $M(\eta_c)$ invariant mass distribution for events in the M_{bc} and ΔE signal region. Signals at the η_c and J/ψ masses from $B \rightarrow \eta_c K$ and $B \rightarrow J/\psi K$ decays are visible.

The contributions to the systematic error include the uncertainties due to the tracking efficiency (2% per track), particle identification efficiency (4-14%, depending on the mode) and the modeling of the likelihood ratio requirement (2%). The error in kaon identification efficiency is obtained from kinematically selected

$D^{*+} \rightarrow D^0\pi^+$, $D^0 \rightarrow K^-\pi^+$ in the data while the error in proton/antiproton identification is determined using $\Lambda/\bar{\Lambda}$ samples. The systematic error due to the modeling of the likelihood ratio cut is determined using $B^+ \rightarrow \bar{D}^0\pi^+$ events reconstructed in data. The systematic error in the yields of the M_{bc} fit were determined by varying the mean and σ of the signal and the shape parameters of the background. To account for the possibility of background from non-resonant modes that may contribute to the M_{bc} distribution, we include the yields observed in the η_c mass sideband (8-14% of the signal depending on the mode) as an asymmetric systematic error. The sources of systematic error are combined in quadrature to obtain the total systematic error, which is given in Table II.

TABLE I. Signal yields from M_{bc} and ΔE fits, statistical significances and MC reconstruction efficiencies. Errors are statistical only.

$B^+ \rightarrow \eta_c K^+$	ΔE Yield	M_{bc} Yield	Signif. (M_{bc})	ϵ (%)
$\eta_c \rightarrow K_S^0 K^- \pi^+$	74.8 ± 10.4	81.6 ± 10.3	12.2σ	16.4
$\eta_c \rightarrow K^+ K^- \pi^0$	26.5 ± 7.8	31.8 ± 7.0	6.3σ	8.8
$\eta_c \rightarrow p\bar{p}$	16.3 ± 4.2	17.7 ± 4.4	7.5σ	34.0
$\eta_c \rightarrow K^{*0} K^- \pi^+$	22.0 ± 5.8	20.8 ± 5.4	5.8σ	5.1

$B^0 \rightarrow \eta_c K_S^0$	ΔE Yield	M_{bc} Yield	Signif. (M_{bc})	ϵ (%)
$\eta_c \rightarrow K_S^0 K^- \pi^+$	19.6 ± 5.4	23.0 ± 5.4	6.8σ	15.5
$\eta_c \rightarrow K^+ K^- \pi^0$	19.9 ± 5.7	17.1 ± 5.1	4.7σ	9.5
$\eta_c \rightarrow p\bar{p}$	7.0 ± 3.0	6.8 ± 2.6	5.0σ	34.9
$\eta_c \rightarrow K^{*0} K^- \pi^+$	0.2 ± 1.7	2.2 ± 1.8	1.6σ	3.75

TABLE II. Product branching fractions for $B \rightarrow \eta_c K$ decay modes (10^{-6}).

$\mathcal{B}(B^+ \rightarrow \eta_c K^+) \times \mathcal{B}(\eta_c \rightarrow K_S^0 K^- \pi^+)$	$(23.2 \pm 2.9^{+2.8}_{-3.8})$
$\mathcal{B}(B^+ \rightarrow \eta_c K^+) \times \mathcal{B}(\eta_c \rightarrow K^+ K^- \pi^0)$	$(11.4 \pm 2.5^{+1.1}_{-1.8})$
$\mathcal{B}(B^+ \rightarrow \eta_c K^+) \times \mathcal{B}(\eta_c \rightarrow p\bar{p})$	$(1.64 \pm 0.41^{+0.17}_{-0.24})$
$\mathcal{B}(B^+ \rightarrow \eta_c K^+) \times \mathcal{B}(\eta_c \rightarrow K^{*0} K^- \pi^+)$	$(19.3 \pm 5.0^{+3.4}_{-3.8})$
$\mathcal{B}(B^0 \rightarrow \eta_c K^0) \times \mathcal{B}(\eta_c \rightarrow K_S^0 K^- \pi^+)$	$(20.1 \pm 4.7^{+3.0}_{-4.5})$
$\mathcal{B}(B^0 \rightarrow \eta_c K^0) \times \mathcal{B}(\eta_c \rightarrow K^+ K^- \pi^0)$	$(16.6 \pm 5.0^{+1.8}_{-1.8})$
$\mathcal{B}(B^0 \rightarrow \eta_c K^0) \times \mathcal{B}(\eta_c \rightarrow p\bar{p})$	$(1.79 \pm 0.68^{+0.19}_{-0.25})$
$\mathcal{B}(B^0 \rightarrow \eta_c K^0) \times \mathcal{B}(\eta_c \rightarrow K^{*0} K^- \pi^+)$	$(8.1 \pm 6.6 \pm 1.4)$
	< 29 at 90% C.L.

The product branching fractions are given in Table II for all modes in which signals are observed. Since many of the η_c branching fractions are poorly determined and in some cases there are conflicting measurements, we quote B branching fractions for the $\eta_c \rightarrow K_S^0 K^- \pi^+$ and $\eta_c \rightarrow K^- K^+ \pi^0$ modes only. The $\eta_c \rightarrow K_S^0 K^- \pi^+$ mode is the most precisely and reliably measured mode and the

branching fraction for the $\eta_c \rightarrow K^- K^+ \pi^0$ mode is related by isospin. We use $\mathcal{B}(\eta_c \rightarrow K_S^0 K^- \pi^+) = 1/3 \times (0.055 \pm 0.017)$ where $1/3$ is the appropriate Clebsch-Gordon coefficient. We assume that the experimental systematic errors in the $\eta_c \rightarrow K_S^0 K^- \pi^+$ and $\eta_c \rightarrow K^- K^+ \pi^0$ modes are uncorrelated. We assume equal production of $B^+ B^-$ and $B^0 \bar{B}^0$ pairs and do not include an additional systematic error for the uncertainty in this assumption. We find

$$\mathcal{B}(B^+ \rightarrow \eta_c K^+) = (1.25 \pm 0.14^{+0.10}_{-0.12} \pm 0.38) \times 10^{-3}$$

and

$$\mathcal{B}(B^0 \rightarrow \eta_c K^0) = (1.23 \pm 0.23^{+0.12}_{-0.16} \pm 0.38) \times 10^{-3}.$$

The first error is statistical, the second error is systematic and the third error is due to the uncertainty in the η_c branching fraction scale. When the η_c branching fractions for the other modes are better determined, absolute B branching fractions for these modes can be extracted from our results.

In the $B^0 \rightarrow \eta_c K^{*0}$, $K^{*0} \rightarrow K^+ \pi^-$ channel, the η_c is reconstructed in the $K_S^0 K^\pm \pi^\mp$ mode. Since this mode is a pseudoscalar to pseudoscalar-vector decay, by angular momentum conservation, the cosine of the K^* helicity angle ($\cos \theta_H$) follows a $\cos^2 \theta_H$ distribution; we select events with $|\cos \theta_H| > 0.4$. We also investigate $B\bar{B}$ background and find that this background can be removed by applying vetos to events with combinations that are consistent with $J/\psi \rightarrow K_S^0 K\pi$, $J/\psi \rightarrow K^+ K^- \pi^+ \pi^-$, $\psi(2S) \rightarrow K_S^0 K\pi$, $\eta_c(2S) \rightarrow K_S^0 K\pi$, $\chi_{c1} \rightarrow K_S^0 K\pi$, $\eta_c \rightarrow K^+ K^- \pi^+ \pi^-$, $D_s^+ \rightarrow K_S^0 K^+$ and $D_s \rightarrow K^- K^+ \pi$. The detection efficiency for these selection requirements is $(7.95 \pm 0.12)\%$.

After applying these requirements, a fit to the M_{bc} distribution yields a signal of 33.7 ± 6.7 events for $B^0 \rightarrow \eta_c K^{*0}$ with a statistical significance of 7.7σ . The M_{bc} distribution is shown in Fig. 3(a). The yields from the ΔE fit, shown in Fig. 3(b) (30 ± 7 events), the η_c invariant mass distribution (24 ± 7 events) and the $K^+ \pi^-$ invariant mass distribution (27 ± 8 events) are consistent with the yield from the M_{bc} fit.

To evaluate the contribution from non-resonant $B^0 \rightarrow K_S^0 K^+ \pi^- K^*$ as well as the remaining $B\bar{B}$ backgrounds that peak in the M_{bc} distribution, we select events in the η_c sideband [13] and repeat the M_{bc} fit. We find no significant signal. By using the ratio of the yields in the η_c signal and sideband regions determined from MC, we estimate the contributions of such backgrounds to be 3.9 ± 4.2 events, consistent with zero. We use the K^* sideband [13] to estimate the non-resonant $B^0 \rightarrow \eta_c K\pi$ decay component and obtain -0.6 ± 3.3 events. These possible background contributions are not subtracted in the branching fraction measurement, but instead are treated as systematic uncertainties. We find

$$\mathcal{B}(B^0 \rightarrow \eta_c K^{*0}) = (1.62 \pm 0.32^{+0.24}_{-0.34} \pm 0.50) \times 10^{-3}.$$

To take into account the possibility of $B\bar{B}$ background, we conservatively include asymmetric systematic errors from the results of the fits to the η_c (-12%) and K^* (-8%) sidebands. Other sources of systematic error are the uncertainties in the track reconstruction efficiency ($\pm 2\%$ per track), the parameters in the M_{bc} fit ($\pm 7\%$), particle identification ($\pm 6\%$) and the number of $B^0\bar{B}^0$ events.

From the results for the branching fractions for $B^0 \rightarrow \eta_c K^0$ and $B^0 \rightarrow \eta_c K^{*0}$ determined above, we can determine the ratio $R_{\eta_c} = \mathcal{B}(B^0 \rightarrow \eta_c K^{*0})/\mathcal{B}(B^0 \rightarrow \eta_c K^0)$. The uncertainty from the η_c branching fraction scale cancels in the ratio. We find

$$R_{\eta_c} = 1.33 \pm 0.36^{+0.24}_{-0.33}.$$

Our result can be compared to calculations of this ratio in models based on factorization and is somewhat higher than the prediction of Gourdin, Keum and Pham of 0.78 [14].

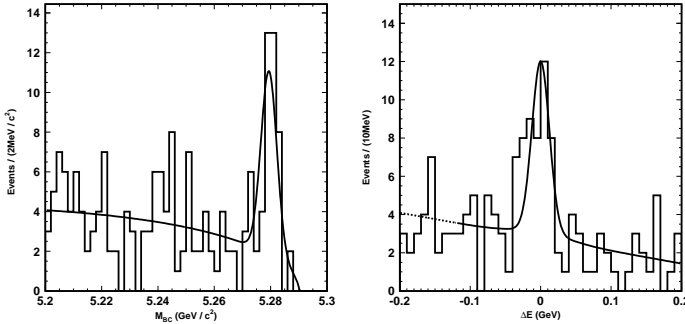


FIG. 3. (a) M_{bc} and (b) ΔE distributions for $B \rightarrow \eta_c K^{*0}$ candidates.

The branching fractions reported in this paper for $B^+ \rightarrow \eta_c K^+$ and $B^0 \rightarrow \eta_c K^0$ using $\eta_c \rightarrow K\bar{K}\pi$ decays are more precise than previous results [15]. The result for the $B^+ \rightarrow \eta_c K^+$ branching fraction is somewhat higher than the CLEO measurement, while the $B^0 \rightarrow \eta_c K^0$ result is consistent. Several additional η_c modes including $\eta_c \rightarrow p\bar{p}$, $\eta_c \rightarrow K^-K^+\pi^0$ and $\eta_c \rightarrow K^{*0}K^-\pi^+$ have been used and increase the fraction of η_c decays that can be reconstructed for CP violation measurements. In addition, we report the first observation of the $B^0 \rightarrow \eta_c K^{*0}$ decay, which is an CP eigenstate when $K^{*0} \rightarrow K_S^0\pi^0$.

We wish to thank the KEKB accelerator group for the excellent operation of the KEKB accelerator. We acknowledge support from the Ministry of Education, Culture, Sports, Science, and Technology of Japan and the Japan Society for the Promotion of Science; the Australian Research Council and the Australian Department of Industry, Science and Resources; the National Science Foundation of China under contract No. 10175071; the Department of Science and Technology of India; the BK21 program of the Ministry of Education of Korea and the CHEP SRC program of the Korea Science and

Engineering Foundation; the Polish State Committee for Scientific Research under contract No. 2P03B 17017; the Ministry of Science and Technology of the Russian Federation; the Ministry of Education, Science and Sport of Slovenia; the National Science Council and the Ministry of Education of Taiwan; and the U.S. Department of Energy.

- [1] K. Abe *et al.* (Belle Collaboration), Phys. Rev. Lett. **87**, 091802 (2001).
- [2] K. Abe *et al.* (Belle Collaboration), hep-ex/0202027, submitted to Phys. Rev. D.
- [3] N.G. Deshpande and J. Trampetic, Phys. Lett. B **339**, 270 (1994).
- [4] The inclusion of the charge conjugate mode is implied.
- [5] KEKB B Factory Design Report, KEK Report 95-1, 1995, unpublished.
- [6] A. Abashian *et al.* (Belle Collaboration.), Nucl. Instr. and Meth. A **479**, 117 (2002).
- [7] The vertex χ^2 requirement is < 50 for all modes except for $\eta_c \rightarrow K_S^0 K^- \pi^+$, where a less restrictive cut < 100 is used.
- [8] The Fox-Wolfram moments were introduced in G.C. Fox and S. Wolfram, Phys. Rev. Lett. **41**, 1581 (1978). The Fisher discriminant used by Belle is described in K. Abe *et al.*, Phys. Rev. Lett. **87**, 101801 (2001) and K. Abe *et al.*, Phys. Lett. B **511**, 151 (2001).
- [9] H. Albrecht *et al.* (ARGUS Collaboration), Phys. Lett. B 241, 278 (1991).
- [10] The significances are calculated from the change in the likelihood when the signal yield is set to zero.
- [11] G.J. Feldman and R.D. Cousins, Phys. Rev. D **57**, 3873 (1998).
- [12] D.E. Groom *et al.* (Particle Data Group), Eur. Phys. J. C **15**, 1 (2000).
- [13] The mass regions $2.74 < M_{K_S K^\pm \pi^\mp} < 2.84 \text{ GeV}/c^2$ and $3.25 < M_{K_S K^\pm \pi^\mp} < 3.35 \text{ GeV}/c^2$ are used as the η_c sideband. The range $1.60 < M_{K^- \pi^+} < 1.79 \text{ GeV}/c^2$ is used as the K^* sideband.
- [14] M. Gourdin, Y. Y. Keum and X.Y. Pham, Phys. Rev. D **51**, 3510 (1996).
- [15] K. Edwards *et al.* (CLEO Collaboration), Phys. Rev. Lett. **86**, 30 (2001).